COMPARISON BETWEEN THE CEBECI AND SMITH AND THE BALDWIN AND LOMAX TURBULENCE MODELS – FINAL RESULTS

Edisson Sávio de Góes Maciel, edissonsavio@yahoo.com.br[1]

[1] Mechanical Engineer/Researcher – Rua Demócrito Cavalcanti, 152 – Afogados – Recife – PE – Brazil – 50750-080

Abstract. *The present work is the final part of the study that aims a comparison between the turbulence models of Cebeci and Smith and of Baldwin and Lomax applied to aeronautical and aerospace problems. The Jameson and Mavriplis algorithm is used to perform the numerical experiments. The algorithm is symmetrical, second order accurate in space and time, and the temporal integration is accomplished by a Runge-Kutta type method. The Reynolds average Navier-Stokes equations are solved, using a finite volume formulation and a structured spatial discretization, and the models of Cebeci and Smith and of Baldwin and Lomax are used to describe the turbulence effects in the flow properties. The physical problems of the transonic flow along a convergent-divergent nozzle and the "cold gas" hypersonic flow around a double ellipse configuration are studied. A spatially variable time step is employed to accelerate the convergence of the numerical scheme. Effective gains in terms of convergence ratio are observed with this technique, as reported in Maciel. The numerical results are compared with experimental or theoretical solutions. These results have demonstrated that the Baldwin and Lomax model is more severe in the nozzle problem, while the Cebeci and Smith model is more severe in the double ellipse problem and more accurate in both examples.*

Keymords: *Algebraic turbulence model of Cebeci and Smith, Algebraic turbulence model of Baldwin and Lomax, Jameson and Mavriplis algorithm, Navier-Stokes equations, Nozzle and double ellipse problems.*

1. INTRODUCTION

The development of aeronautical and aerospace projects require hours of wind tunnel essays. It is necessary to minimize such wind tunnel procedures due to the growing cost of electrical energy. In Brazil, there is the problem of this country has not yet wind tunnels of great capacity, able to generate supersonic flows or even high subsonic flows. So, Computational Fluid Dynamics, CFD, techniques have now great highlight in the aeronautical industry scenario. Analogous to wind tunnel essays, the numerical methods determine physical properties in discrete points of the spatial domain. Hence, the aerodynamic coefficients of lift, drag and momentum can be calculated. A numerical scheme which fulfills well this role of giving data to the project phase is the Jameson and Mavriplis (1986) scheme.

Jameson and Mavriplis (1986) emphasized the substantial cost reduction in the calculations of the Euler equation solutions. The method proposed by Jameson, Schmidt and Turkel (1981) had proved robustness, good accuracy and sufficient sophistication to more complete applications. The objective was apply such scheme to geometries like wing-fuselage, involving engines, missiles and other typical components, to represent a whole airplane. The work emphasized the use of triangular cells which allow a bigger flexibility in the description of complex geometries and become the mesh generation process less expensive. The fluid movement equations were spatially discretized on an unstructured context. The scheme used a finite volume formulation with properties determined at the cell centroids. Artificial dissipation operators were constructed to guarantee second order spatial accuracy to the scheme, except in the proximities of shock waves in which the accuracy was reduced to the first order (Jameson, Schmidt and Turkel, 1981). The time integration used a Runge-Kutta method of five stages.

There is a practical necessity in the aeronautical industry and in other fields of the capability of calculating separated turbulent compressible flows. With the available numerical methods, researches seem able to analyze several separated flows, three-dimensional in general, if an appropriated turbulence model is employed. Simple methods as the algebraic turbulence models of Cebeci and Smith (1970) and of Baldwin and Lomax (1978) supply satisfactory results with low computational cost and allow that the main features of the turbulent flow be detected.

Maciel (2006a), the first part of this study, performed a comparison between the Cebeci and Smith (1970) and the Baldwin and Lomax (1978) models in relation to solution quality and numerical accuracy. The numerical algorithms of MacCormack (1969) and of Jameson and Mavriplis (1986) were implemented, on a finite volume and structured spatial discretization contexts, to perform the numerical experiments. The Reynolds average Navier-Stokes equations were solved. The steady state supersonic flow along a ramp was studied. The results have demonstrated that the Cebeci and Smith (1970) model yielded better quality characteristics and more critical solutions than the Baldwin and Lomax

(1978) model as the MacCormack (1969) scheme was studied. When the Jameson and Mavriplis (1986) scheme was studied, no meaningful differences were perceptible.

In the present work, the continuation of Maciel (2006a), the turbulence models of Cebeci and Smith (1970) and of Baldwin and Lomax (1978) are studied in relation to solution quality and numerical accuracy. The Jameson and Mavriplis (1986) algorithm is implemented, using a finite volume formulation and a structured spatial discretization, to perform the numerical experiments. The Reynolds average Navier-Stokes equations are solved applied to the physical problems of the transonic flow along a convergent-divergent nozzle and the "cold gas" hypersonic flow around a double ellipse configuration. A spatially variable time step is implemented to accelerate the convergence process of the Jameson and Mavriplis (1986) algorithm. Effective gains in terms of convergence ratio are observed with this technique, as reported in Maciel (2005, 2008). The numerical results are compared with experimental or theoretical solutions. The results have demonstrated that the Baldwin and Lomax (1978) model was more severe in the nozzle problem, while the Cebeci and Smith (1970) model was more severe in the double ellipse problem and more accurate in both examples.

2. NAVIER-STOKES EQUATIONS

The equation $\partial/\partial t \int_V Q dV + \int_S \vec{F} \bullet \vec{n} dS = 0$ defines the Navier-Stokes equations in integral and conservative forms. In this equation, Q is the vector of conserved variables written to a Cartesian system, V is the cell volume, $\vec{n}$ is the normal unity vector to each flux face, S is the flux area and $\vec{F}$ represents the sum of the convective and diffusive flux vectors. Definitions to F and Q vectors, as well to viscous stresses and the components of the Fourier heat flux are found in Maciel (2006a).

To the nozzle physical problem, the Navier-Stokes equations are nondimensionalized in relation to the stagnation properties. To the double ellipse physical problem, the Navier-Stokes equations are nondimensionalized in relation to the freestream properties.

The Reynolds number is defined by $\mathbf{Re} = \rho V_{REF} l_{REF} / \mu_M$, being ρ the fluid density, V_{REF} a characteristic flow velocity, l_{REF} a geometry characteristic length and μ_M the fluid molecular viscosity. The matrix system of the Navier-Stokes equations is closed with the state equation of a perfect gas $p = (\gamma - 1)\left[e - 0.5\rho(u^2 + v^2)\right]$, assuming the ideal gas hypothesis. In this last equation, γ is the ratio of specific heats, e is the total energy and u and v are the Cartesian flow velocity components.

3. FINITE VOLUMES

Using finite volumes and considering the vector of conserved variables constant in a stationary volume $V_{i,j}$:

$$\partial\left(V_{i,j}Q_{i,j}\right)/\partial t + \int_S \left(\vec{F} \bullet \vec{n}\right)_{i,j} dS_{i,j} = 0. \tag{1}$$

The cell volume and the area components at interface are defined in Maciel (2002) and in Maciel (2006b). Each cell is defined by the nodes *(i,j)*, *(i+1,j)*, *(i+1,j+1)* and *(i,j+1)*. The spatial discretization gives:

$$d\left(V_{i,j}Q_{i,j}\right)/dt + \left[\left(\vec{F} \bullet \vec{S}\right)_{i,j-1/2} + \left(\vec{F} \bullet \vec{S}\right)_{i+1/2,j} + \left(\vec{F} \bullet \vec{S}\right)_{i,j+1/2} + \left(\vec{F} \bullet \vec{S}\right)_{i-1/2,j}\right] = 0. \tag{2}$$

The gradients of the primitive variables are calculated using the Green theorem which considers that the gradient of a primitive variable is constant in the volume and that the volume integral which defines the gradient is replaced by a surface integral (Long, Khan and Sharp, 1991, Maciel, 2002, Maciel, 2006a, and Maciel, 2006b).

4. JAMESON AND MAVRIPLIS (1986) ALGORITHM

Equation (2) can be rewritten on a structured spatial discretization context (Jameson, Schmidt and Turkel, 1981, Jameson and Mavriplis, 1986, and Maciel, 2002) as:

$$d\left(V_{i,j}Q_{i,j}\right)/dt + C(Q_{i,j}) = 0, \tag{3}$$

where:

$$C(Q_{i,j}) = \left[E(Q_{i,j-1/2})S_{x_{i,j-1/2}} + F(Q_{i,j-1/2})S_{y_{i,j-1/2}}\right] + \left[E(Q_{i+1/2,j})S_{x_{i+1/2,j}} + F(Q_{i+1/2,j})S_{y_{i+1/2,j}}\right] +$$
$$\left[E(Q_{i,j+1/2})S_{x_{i,j+1/2}} + F(Q_{i,j+1/2})S_{y_{i,j+1/2}}\right] + \left[E(Q_{i-1/2,j})S_{x_{i-1/2,j}} + F(Q_{i-1/2,j})S_{y_{i-1/2,j}}\right] \tag{4}$$

is the discrete approximation of the flux integral of Eq. (2). E and F are the Cartesian flux components, involving convective and diffusive contributions and S_x and S_y are the Cartesian area components. In this work, it was adopted, for example, that the value of the conserved variables at interface (i,j-1/2) is obtained by arithmetical average between the values of the conserved variables at the (i,j) volume and of the conserved variables at the (i,j-1) volume.

The spatial discretization proposed by the authors is equivalent to a symmetrical scheme with second order accuracy, on a finite difference context. The introduction of a "D" dissipation operator is necessary to guarantee numerical stability in presence of, for example, uncoupled solutions and non-linear instabilities, like shock waves. So, Equation (3) is rewritten as:

$$d\left(V_{i,j}Q_{i,j}\right)/dt + \left[C(Q_{i,j}) - D(Q_{i,j})\right] = 0 . \tag{5}$$

The time integration is performed by a Runge-Kutta explicit method of five stages, second order accurate, and is described in Maciel (2002), in Maciel (2006a) and in Maciel (2006b). The artificial dissipation operator implemented with the Jameson and Mavriplis (1986) scheme is the same as that used in Maciel (2006a) and details are found in Maciel (2002) and in Maciel (2006b).

5. TURBULENCE MODEL OF CEBECI AND SMITH (1970)

The problem of the turbulent simulation is in the calculation of the Reynolds stress. Expressions involving velocity fluctuations, originating from the average process, represent six new unknowns. However, the number of equations keeps the same and the system is not closed. The modeling function is to develop approximations to these correlations. To the calculation of the turbulent viscosity according to the Cebeci and Smith (1970) model, the boundary layer is divided in internal and external.

Initially, the (ν_w) wall fluid cinematic viscosity and the ($\tau_{xy,w}$) wall shear stress are calculated. After that, the (δ) boundary layer thickness, the (δ_{LM}) linear momentum thickness and the (Vt_{BL}) boundary layer tangential velocity are calculated. So, the (N) normal distance from the wall to the studied cell is calculated. The N^+ term is obtained from $N^+ = \sqrt{\mathbf{Re}}\sqrt{\tau_{xy,w}/\rho_w}\ N/\nu_w$, where ρ_w is the wall fluid density. The van Driest damping factor is calculated by:

$$D = 1 - e^{(-N^+\sqrt{\rho/\rho_w}\,\mu_w/\mu/A^+)} , \tag{6}$$

with $A^+ = 26$ and μ_w is the wall fluid molecular viscosity. After that, the (dVt/dN) normal to the wall gradient of the tangential velocity is calculated and the internal turbulent viscosity is given by:

$$\mu_{Ti} = \mathbf{Re}\,\rho(\kappa ND)^2\,dVt/dN , \tag{7}$$

where κ is the von Kárman constant, which has the value 0.4. The intermittent function of Klebanoff is calculated to the external viscosity by $g_{Kleb}(N) = \left[1 + 5.5(N/\delta)^6\right]^{-1}$. With it, the external turbulent viscosity is calculated by:

$$\mu_{Te} = \mathbf{Re}(0.0168)\rho Vt_{BL}\delta_{LM}\,g_{Kleb} . \tag{8}$$

Finally, the turbulent viscosity is chosen from the internal and the external viscosities: $\mu_T = MIN(\mu_{Ti}, \mu_{Te})$.

6. TURBULENCE MODEL OF BALDWIN AND LOMAX (1978)

To the calculation of the turbulent viscosity according to the Baldwin and Lomax (1978) model, the boundary layer is again divided in internal and external. In the internal layer,

$$\mu_{Ti} = \rho l_{mix}^2\|\omega\| \quad \text{and} \quad l_{mix} = \kappa N\left(1 - e^{-N^+/A_0^+}\right). \tag{9}$$

In the external layer,

$$\mu_{Te} = \rho\alpha C_{cp}F_{wake}F_{Kleb}(N; N_{\max}/C_{Kleb}), \text{ with } F_{wake} = MIN\left[N_{\max}F_{\max}; C_{wk}N_{\max}U_{dif}^2/F_{\max}\right] \text{ and } F_{\max} = 1/\kappa\left[\underset{N}{MAX}(l_{mix}\|\omega\|)\right]. \tag{10}$$

Hence, $N_{\max}$ is the value of N where $l_{mix}\|\omega\|$ reached its maximum value and l_{mix} is the Prandtl mixture length. The constant values are: $\kappa = 0.4$, $\alpha = 0.0168$, $A_0^+ = 26$, $C_{cp} = 1.6$, $C_{Kleb} = 0.3$ and $C_{wk} = 1$. F_{Kleb} is the intermittent

function of Klebanoff given by $F_{Kleb}(N) = \left[1 + 5.5(C_{Kleb}N/N_{max})^6\right]^{-1}$, $\|\omega\|$ is the vorticity vector magnitude and U_{dif} is the velocity maximum value in the boundary layer case. To free shear layers,

$$U_{dif} = \left(\sqrt{u^2 + v^2}\right)_{max} - \left(\sqrt{u^2 + v^2}\right)_{N=N_{max}} . \tag{11}$$

7. SPATIALLY VARIABLE TIME STEP

The basic idea of this procedure consists in keeping constant the CFL number in all calculation domain, allowing, hence, the use of appropriated time steps to each specific mesh region during the convergence process. Hence, according to the definition of the CFL number, it is possible to write:

$$\Delta t_{i,j} = CFL(\Delta s)_{i,j}/c_{i,j} , \tag{12}$$

where CFL is the "Courant-Friedrichs-Lewy" number to provide numerical stability to the scheme; $c_{i,j} = \left[\left(u^2 + v^2\right)^{0.5} + a\right]_{i,j}$ is the maximum characteristic speed of propagation of information in the calculation domain; a is the speed of sound, defined as $a = \sqrt{\gamma p/\rho}$; and $(\Delta s)_{i,j}$ is a characteristic length of transport of information. On a finite volume context, $(\Delta s)_{i,j}$ is chosen as the minor value found between the minor centroid distance, involving the *(i,j)* cell and a neighbor, and the minor cell side length.

8. INITIAL AND BOUNDARY CONDITIONS

8.1. Initial Conditions

Stagnation values are used as initial condition to the nozzle problem. Only at the exit boundary is imposed a reduction of 1/3 to the density and to the pressure to start the flow along the nozzle (Maciel, 2002). The vector of conserved variables is defined as:

a) Domain except the nozzle exit (through the nondimensionalization employed in this work)

$$Q = \{1 \quad 0 \quad 0 \quad (\gamma+1)/[2\gamma(\gamma-1)]\}^T ; \tag{13}$$

b) Nozzle exit:

$$Q = \{1/3 \quad 0 \quad 0 \quad (\gamma+1)/[6\gamma(\gamma-1)]\}^T . \tag{14}$$

To the double ellipse problem, values of freestream flow are adopted for all properties as initial condition, in the whole calculation domain (Jameson and Mavriplis, 1986, and Maciel, 2002):

$$Q_\infty = \{1 \quad M_\infty \cos\theta \quad M_\infty sen\theta \quad [1/[\gamma(\gamma-1)] + 0.5M_\infty^2]\}^T , \tag{15}$$

where θ is the flow attack angle and M_∞ is the freestream Mach number.

8.2. Boundary Conditions

The different types of boundary conditions implemented in this work are described in Maciel (2002) and in Maciel (2006a,b).

9. RESULTS

Tests were performed in a CELERON-1.2 GHz and 128 Mbytes of RAM memory microcomputer. Converged results occurred to 3 orders of reduction in the value of the maximum residual. The value used to γ was 1.4. The attack angle was adopted equals to 0.0°. The values of the Prandtl numbers are: 0.72 to the molecular and 0.9 to the turbulent.

9.1. Convergent-Divergent Nozzle Problem – Laminar Solution

An algebraic mesh of 61x71 points, with an exponential stretching of 10% in both ξ and η directions, was used. It is equivalent to be composed of 4,200 rectangular volumes and 4,331 nodes. The Reynolds number was estimated in 652,210.2, to an altitude of 0.0m and a characteristic length of $l = 0.028$m, based on Fox and McDonald (1988) data.

Figures 1 and 2 exhibit the density and the pressure fields to the laminar flow generated by the Jameson and Mavriplis (1986) scheme. Pressure oscillations in the pressure field do not occur.
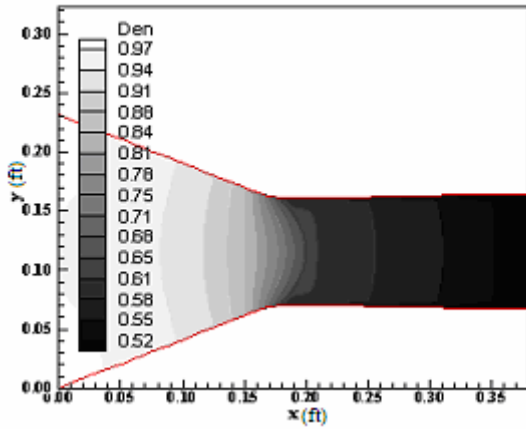
Figure 1. Density field (L).
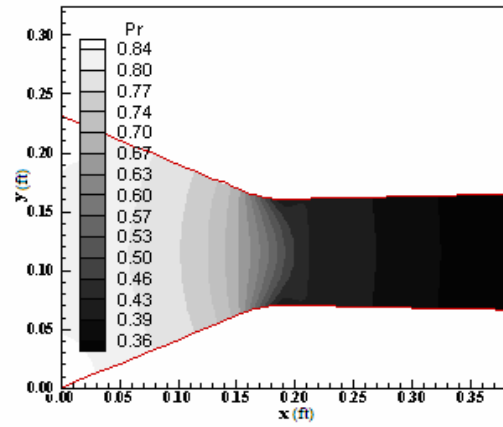
Figure 2. Pressure field (L).

Figures 3 and 4 exhibit the Mach number contours and the pressure distribution along the nozzle lower wall, respectively. Figure 3 does not present pre-shock oscillations near the throat. The pressure distribution along the nozzle lower wall, Fig. 4, exhibits the shock at the throat. This shock has a pressure ratio value equals to 0.5.
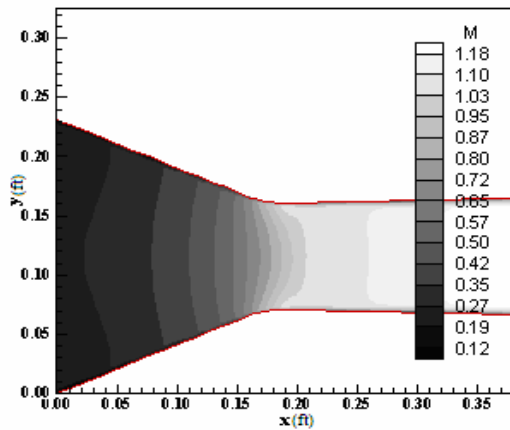
Figure 3. Mach number field (L).
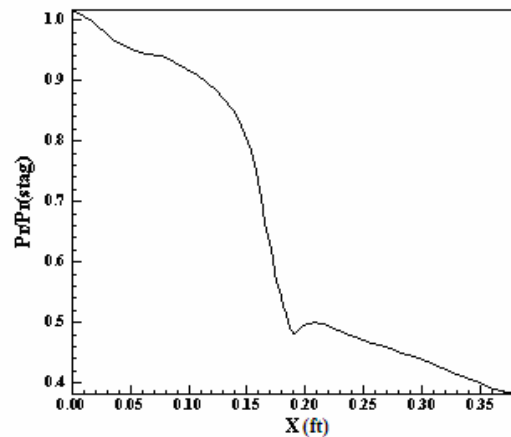
Figure 4. Wall pressure distribution (L).

9.2. Convergent-Divergent Nozzle Problem – Turbulent Solutions

Figures 5 and 6 exhibit the density field of the turbulent flow obtained with the Cebeci and Smith (1970) and with the Baldwin and Lomax (1978) models, respectively. The density peaks generated by the turbulent solutions are the same than the respective peak generated by the laminar solution. The field generated by the Baldwin and Lomax (1978) model is denser than the field obtained by the Cebeci and Smith (1970) model.

Figures 7 and 8 exhibit the pressure contours to the turbulent flow. The pressure filed generated by the Baldwin and Lomax (1978) model is lightly more severe than the respective field generated by the Cebeci and Smith (1970) model.

Figures 9 and 10 exhibit the Mach number contours generated by both models. The field generated by the Cebeci and Smith (1970) model is more intense than that generated by the Baldwin and Lomax (1978) model.

Figure 11 exhibits the pressure distributions along the nozzle lower wall generated by the laminar and the turbulence models of Cebeci and Smith (1970) and of Baldwin and Lomax (1978). All solutions are compared with the experimental results of Mason, Putnam and Re (1980). As can be seen, the shock detected by the Baldwin and Lomax (1978) model is more severe than that detected by the Cebeci and Smith (1970) model. The pressure ratio at the shock calculated by the Baldwin and Lomax (1978) model has a value of 0.5, according to the laminar solution, while the same pressure ratio calculated by the Cebeci and Smith (1970) model has a value of 0.48. However, the Cebeci and Smith (1970) solution is the closest with the experimental results. Hence, the Baldwin and Lomax (1978) model presents more severe and critical solutions than the Cebeci and Smith (1970) model, to this physical problem, although the Cebeci and Smith (1970) is more accurate in terms of pressure distribution, closer to the experimental results.
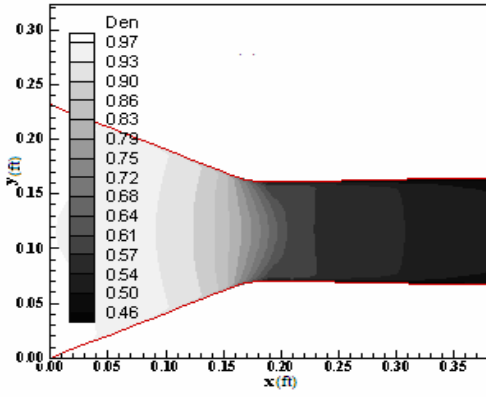
Figure 5. Density field (CS).
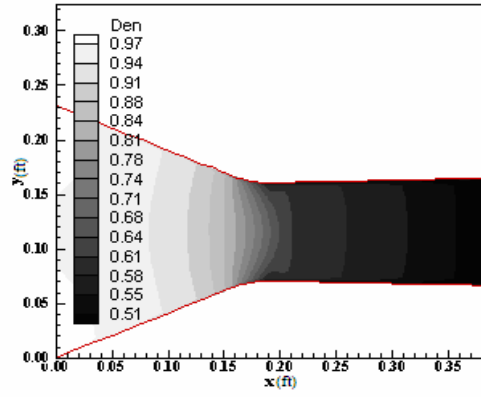
Figure 6. Density field (BL).
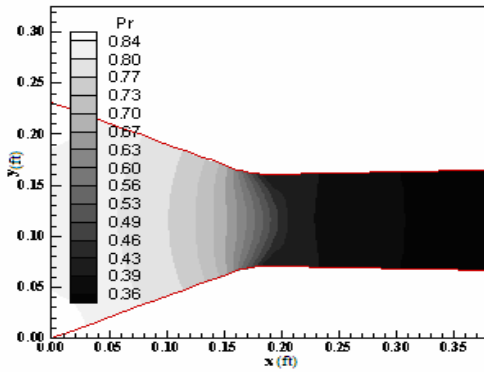
Figure 7. Pressure field (CS).
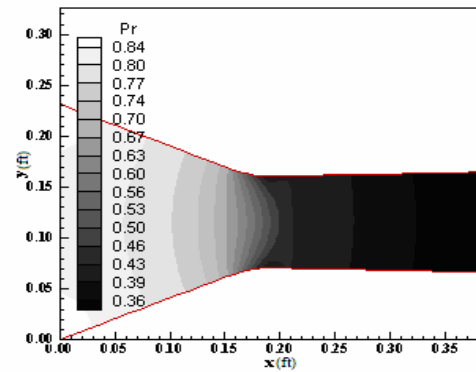
Figure 8. Pressure field (BL).
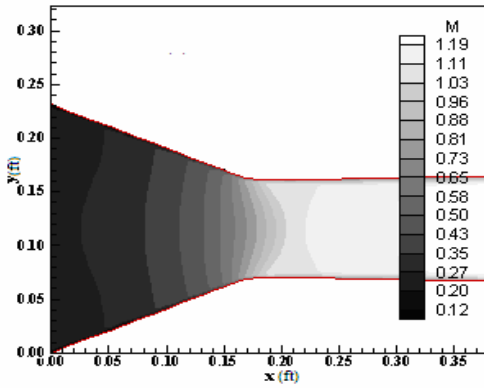
Figure 9. Mach number field (CS).
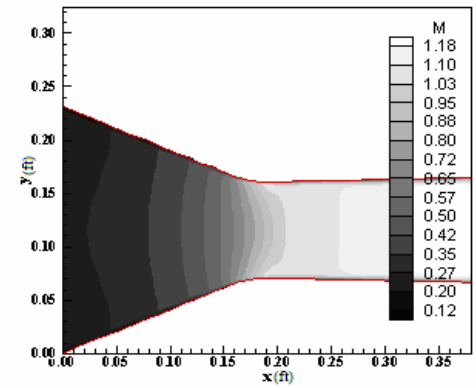
Figure 10. Mach number field (BL).
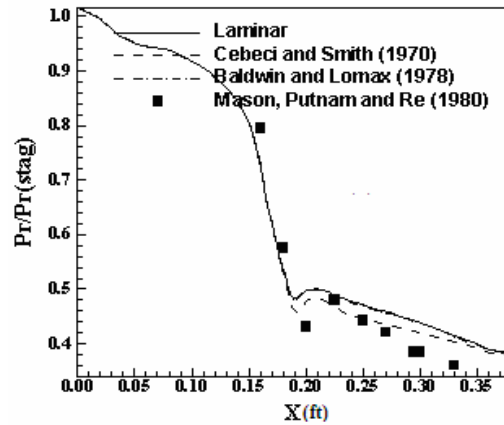
Figure 11. Lower wall pressure distributions.

9.3. Double Ellipse Problem – Laminar Solution

An algebraic mesh of 125x70 points, with an exponential stretching of 10% in the η direction, was used. It is equivalent to be composed of 8,556 rectangular volumes and 8,750 nodes. A freestream Mach number of 10.0 was adopted as initial condition. The Reynolds number was estimated in 3,959,821.0, to an altitude of 40,000m and a characteristic length of $l = 5.0$m, based on Fox and McDonald (1988) data.

Figures 12 and 13 exhibit the density and the pressure fields to the laminar flow generated by the Jameson and Mavriplis (1986) scheme. The pressure field does not present pressure oscillations. Figures 14 and 15 exhibit the Mach number contours and the -Cp distribution around the double ellipse, respectively. Figure 14 does not present pre-shock oscillations. The -Cp distribution around the double ellipse, Fig. 15, exhibits the two shocks, at the configuration nose and at the second ellipse. The Cp value of the first shock is equal to 1.76, while the second shock has a value of 0.92.
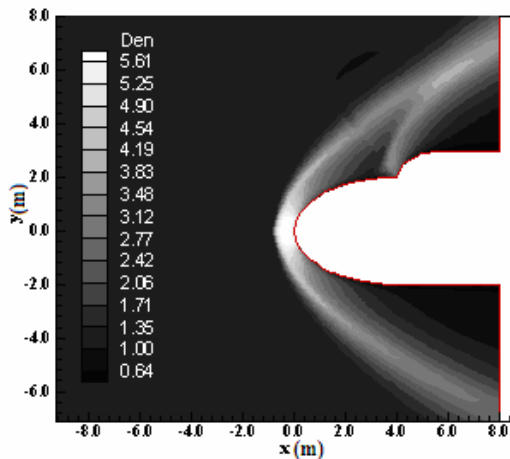
Figure 12. Density field (L).
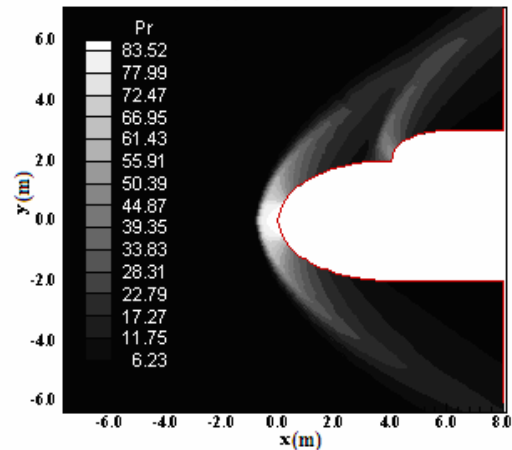
Figure 13. Pressure field (L).
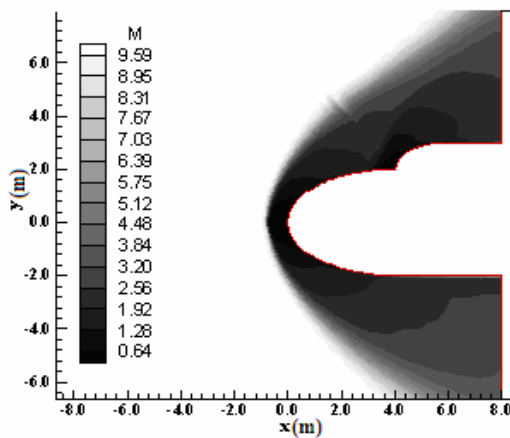
Figure 14. Mach number field (L).
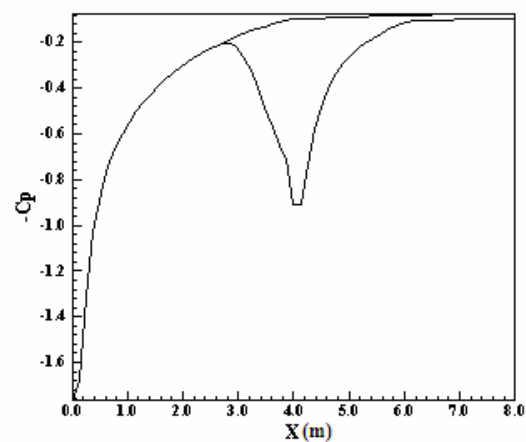
Figure 15. -Cp distribution (L).

The lift and drag aerodynamic coefficients calculated to the laminar case are: $c_L = -1,213 \times 10^{-1}$ and $c_D = -2,541 \times 10^{-3}$. Only pressure effects are considered in the determination of these coefficients. In this problem, the aerodynamic coefficients should have values different from zero and the c_L coefficient should have a negative value because the second shock originates a normal resultant pointing downwards over the double ellipse.

9.4. Double Ellipse Problem – Turbulent Solutions

Figures 16 and 17 exhibit the density field of the turbulent flow obtained with the Cebeci and Smith (1970) and with the Baldwin and Lomax (1978) models, respectively. The density peaks generated by the turbulent solutions are less intense than the respective peak generated by the laminar solution. The field obtained by the Baldwin and Lomax (1978) model is denser than the field generated by the Cebeci and Smith (1970) model.

Figures 18 and 19 exhibit the pressure contours to the turbulent flow. The pressure field obtained by the Cebeci and Smith (1970) model is more severe than that generated by the Baldwin and Lomax (1978) model.

Figures 20 and 21 exhibit the Mach number contours generated by the models. The field generated by the Baldwin and Lomax (1978) scheme is more intense than that generated by the Cebeci and Smith (1970) model.
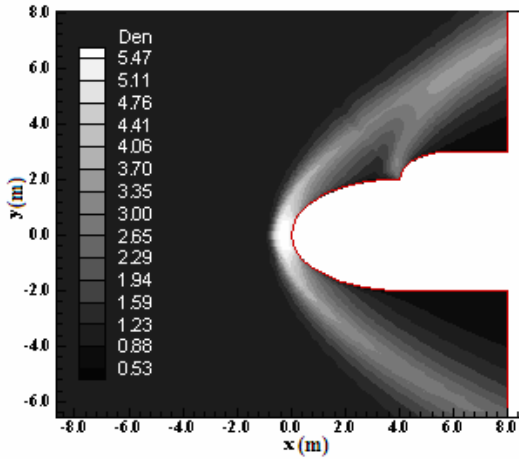
Figure 16. Density field (CS).
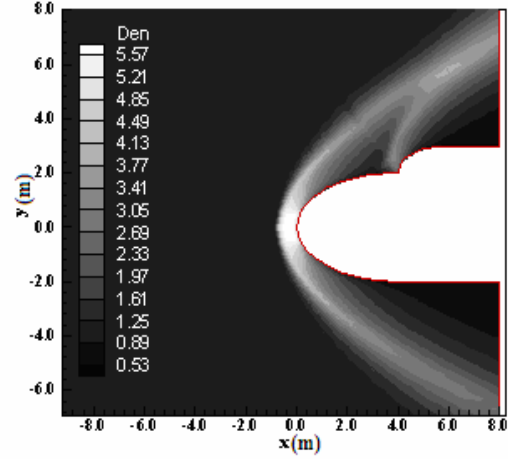
Figure 17. Density field (BL).
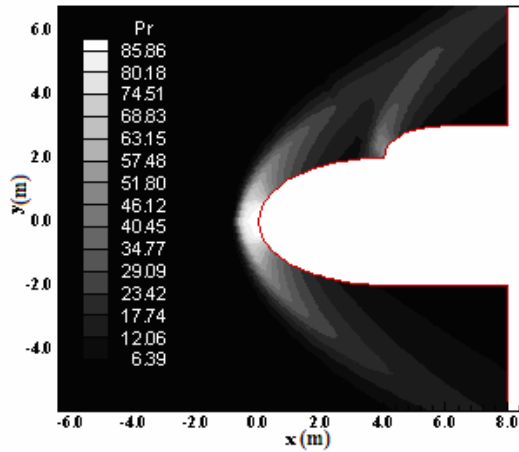
Figure 18. Pressure field (CS).
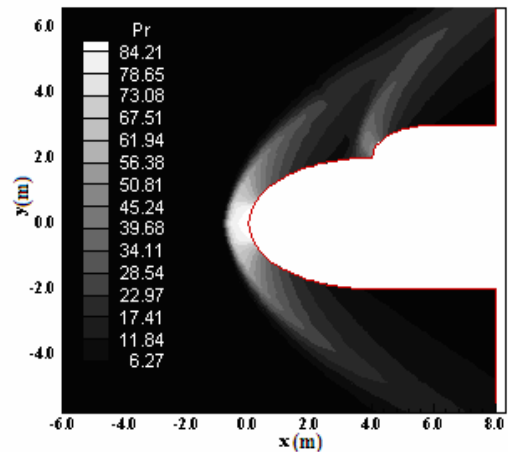
Figure 19. Pressure field (BL).
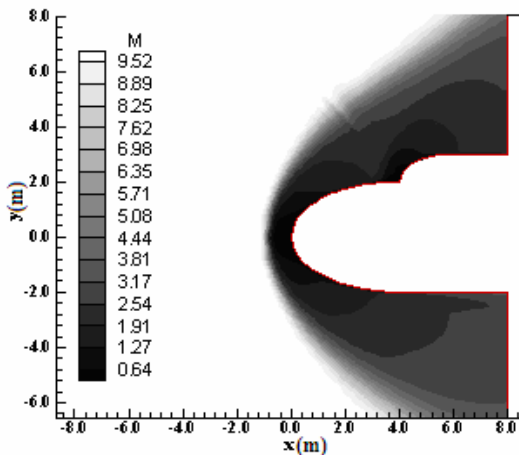
Figure 20. Mach number field (CS).
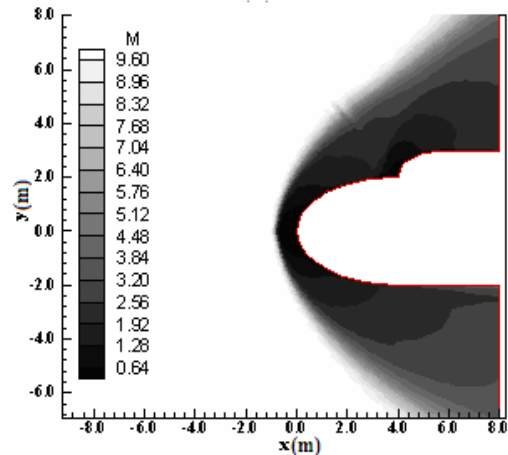
Figure 21. Mach number field (BL).

Figure 22 exhibits the -Cp distributions around the double ellipse generated by the laminar and the turbulence models of Cebeci and Smith (1970) and of Baldwin and Lomax (1978). Both turbulence models detect the two shocks, at the configuration nose and the second ellipse. The first shock has a Cp value of 1.82 by the Cebeci and Smith (1970) model and of 1.78 by the Baldwin and Lomax (1978) model. The second shock presents the following Cp values: Cp = 0.94 by the Cebeci and Smith (1970) model and Cp = 0.92 by the Baldwin and Lomax (1978) model. So, the Cebeci and Smith (1970) model presents Cp values at the two shocks more severe than the Baldwin and Lomax (1978) model.
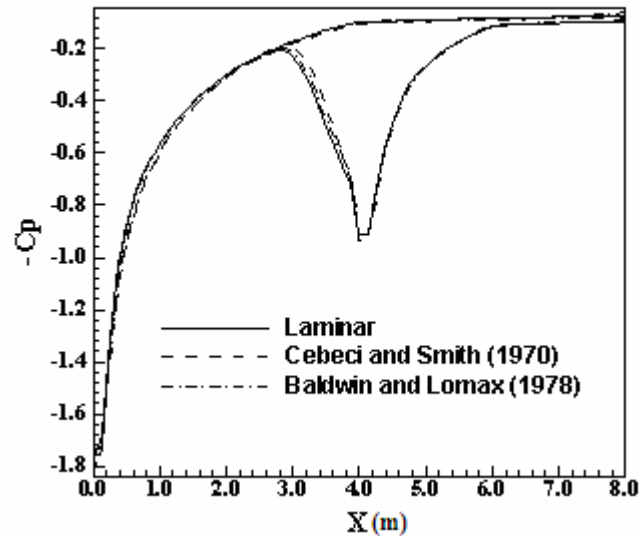
Figure 22. -Cp distributions.

Table 1 shows the lift and drag aerodynamic coefficients calculated to the turbulent case. Only pressure effects are considered in the determination of these coefficients. As can be seen, the Baldwin and Lomax (1978) model presents more severe and bigger values (in modulus) of c_L and c_D than the Cebeci and Smith (1970) model, although these values are smaller than the respective values of the laminar solution.

Table 1. Aerodynamic coefficients – Turbulent case.

Model	c_L	c_D
Cebeci and Smith (1970)	$-1,117 \times 10^{-1}$	$1,456 \times 10^{-3}$
Baldwin and Lomax (1978)	$-1,180 \times 10^{-1}$	$-2,270 \times 10^{-3}$

Another possibility to quantitative comparison of both schemes is the determination of the stagnation pressure ahead of the configuration. Anderson Jr. (1984) presents a table of normal shock wave properties in its B Appendix. This table permits the determination of some shock wave properties as function of the freestream Mach number. In front of the double ellipse configuration studied in this work, the shock wave presents a normal shock behavior, which permits the determination of the stagnation pressure, behind the shock wave, from the tables encountered in Anderson Jr. (1984). So it is possible to determine the ratio pr_0/pr_∞ from Anderson Jr. (1984), where pr_0 is the stagnation pressure in front of the configuration and pr_∞ is the freestream pressure (equals to $1/\gamma$ to the present nondimensionalization).

Hence, to this problem, $M_\infty = 10.0$ corresponds to $pr_0/pr_\infty = 129.2$ and remembering that $pr_\infty = 0.714$, it is possible to conclude that $pr_0 = 92.25$. Table 2 presents values of the stagnation pressure and of the percentage errors obtained by each turbulence model. As can be seen, the Cebeci and Smith (1970) model is more accurate than the Baldwin and Lomax (1978) model to this problem.

Table 2. Values of stagnation pressure and percentage errors to each turbulence model.

Model	pr_0	Error (%)
Cebeci and Smith (1970)	85.86	6.9
Baldwin and Lomax (1978)	84.21	8.7

9.5. Computational Data of the Simulations

Table 3. Numerical data of the nozzle and double ellipse simulations.

Model	Nozzle		Double ellipse		
	CFL	Iterations	CFL	Iterations	Cost*
Laminar	2.5	838	0.4	2,461	0.0000334
Cebeci and Smith (1970)	0.1	29,228	0.4	1,996	0.0001507
Baldwin and Lomax (1978)	2.6	821	0.4	2,029	0.0000858

* Given in second/per volume/per iteration

Table 3 shows the numerical data of the laminar and turbulent simulations. The Jameson and Mavriplis (1986) cost had an increase of 351% with the implementation of the Cebeci and Smith (1970) model in relation to the laminar solution, while with the Baldwin and Lomax (1978) model this increase was of 157%.

10. CONCLUSIONS

In the present work, the continuation of Maciel (2006a), the turbulence models of Cebeci and Smith (1970) and of Baldwin and Lomax (1978) were studied in the solution of the turbulent transonic flow along a convergent-divergent nozzle and of the turbulent "cold gas" hypersonic flow around a double ellipse configuration. The Jameson and Mavriplis (1986) algorithm, using a finite volume formulation and a structured spatial discretization, was employed to numerical experiments. The Reynolds average Navier-Stokes equations were solved and the Cebeci and Smith (1970) and the Baldwin and Lomax (1978) models were used to simulate the effects of the turbulent flow. A spatially variable time step was implemented aiming to accelerate the convergence process. The effective gains in terms of convergence ratio are reported in Maciel (2005, 2008).

The results have demonstrated that the Baldwin and Lomax (1978) model was more severe in the nozzle problem, while the Cebeci and Smith (1970) model was more severe in the double ellipse problem and more accurate in both examples. In the nozzle problem, the Baldwin and Lomax (1978) model predicts a pressure field more severe than the Cebeci and Smith (1970) model. However, the wall pressure distribution and the pressure ratio at the shock are better described and estimated by the Cebeci and Smith (1970) model. In the double ellipse problem, the pressure field is more severe in the solution obtained by the Cebeci and Smith (1970) model. The density and the Mach number fields are denser and more intense, respectively, in the solution obtained by the Baldwin and Lomax (1978) model. However, the Cp values of the two shocks, at the configuration nose and at the second ellipse, are more severe in the solution obtained by the Cebeci and Smith (1970) model. Moreover, a more accurate solution is obtained by the Cebeci and Smith (1970) model in the determination of the stagnation pressure in front of the configuration nose, although more severe values of c_L and c_D are calculated by the Baldwin and Lomax (1978) model. The computational cost of the Jameson and Mavriplis (1986) scheme using the turbulence model of Cebeci and Smith (1970) is 351% more expensive than the laminar solution, while the Baldwin and Lomax (1978) model is only 157% more expensive.

11. REFERENCES

Anderson Jr., J. D., 1984, "Fundamentals of Aerodynamics", McGraw-Hill, Inc., EUA, 563p.

Baldwin, B. S., and Lomax, H., 1978, "Thin Layer Approximation and Algebraic Model for Separated Turbulent Flows", AIAA Paper 78-257.

Cebeci, T., and Smith, A. M. O., 1970, "A Finite-Difference Method for Calculating Compressible Laminar and Turbulent Boundary Layers", Journal of Basic Engineering, Trans. ASME, Series B, Vol. 92, No. 3, September, pp. 523-535.

Fox, R. W. and McDonald, A. T., 1988, "Introdução à Mecânica dos Fluidos", Ed. Guanabara Koogan, Rio de Janeiro, RJ, Brazil, 632p.

Jameson, A. and Mavriplis, D. J., 1986, "Finite Volume Solution of the Two-Dimensional Euler Equations on a Regular Triangular Mesh", AIAA Journal, Vol. 24, No. 4, pp. 611-618.

Jameson, A., Schmidt, W. and Turkel, E., 1981, "Numerical Solution for the Euler Equations by Finite Volume Methods Using Runge-Kutta Time Stepping Schemes", AIAA Paper 81-1259.

Long, L. N., Khan, M. M. S. and Sharp, H. T., 1991, "Massively Parallel Three-Dimensional Euler / Navier-Stokes Method", AIAA Journal, Vol. 29, No. 5, pp. 657-666.

MacCormack, R. W., 1969, "The Effect of Viscosity in Hypervelocity Impact Cratering", AIAA Paper 69-354.

Maciel, E. S. G., 2002, "Simulação Numérica de Escoamentos Supersônicos e Hipersônicos Utilizando Técnicas de Dinâmica dos Fluidos Computacional", Doctoral thesis, ITA, CTA, São José dos Campos, SP, Brasil, 258 p.

Maciel, E. S. G., 2005, "Analysis of Convergence Acceleration Techniques Used in Unstructured Algorithms in the Solution of Aeronautical Problems – Part I", Proceedings of the XVIII International Congress of Mechanical Engineering (XVIII COBEM), Ouro Preto, MG, Brazil.

Maciel, E. S. G., 2006a, "Comparação entre os Modelos de Turbulência de Cebeci e Smith e de Baldwin e Lomax", Proceedings of the 5ª Spring School of Transition and Turbulence (V EPTT), Rio de Janeiro, RJ, Brazil.

Maciel, E. S. G., 2006b, "Estudo de Escoamentos Turbulentos Utilizando os Modelos de Cebeci e Smith e de Baldwin e Lomax e Comparação entre os Algoritmos de MacCormack e de Jameson e Mavriplis", Proceedings of the 7th Symposium of Computational Mechanics (VII SIMMEC), Araxá, MG, Brazil.

Maciel, E. S. G., 2008, "Analysis of Convergence Acceleration Techniques Used in Unstructured Algorithms in the Solution of Aerospace Problems – Part II", Proceedings of the XII Brazilian Congress of Thermal Engineering and Sciences (XII ENCIT), Belo Horizonte, MG, Brazil.

Mason, M. L., Putnam, L. E., and Re, R. J., 1980, "The Effect of Throat Contouring on Two-Dimensional Converging-Diverging Nozzles at Sonic Conditions", NASA Technical Paper 1704.

12. RESPONSIBILITY NOTICE

The author is the only responsible for the printed material included in this paper.